HHS Public Access

Author manuscript

Reprod Toxicol. Author manuscript; available in PMC 2021 December 01.

Published in final edited form as:

Reprod Toxicol. 2020 December ; 98: 61–74. doi:10.1016/j.reprotox.2020.08.010.

Epigenome-Wide Association Study for Transgenerational Disease Sperm Epimutation Biomarkers following Ancestral Exposure to Jet Fuel Hydrocarbons

Millissia Ben Maamar, **Eric Nilsson**, **Jennifer L.M. Thorson**, **Daniel Beck**, **Michael K. Skinner***

Center for Reproductive Biology, School of Biological Sciences, Washington State University, Pullman, WA, 99164-4236, USA

Abstract

Jet fuel hydrocarbons is the generic name for aviation fuels used in gas-turbine engine powered aircraft. The Deepwater Horizon oil rig explosion created the largest environmental disaster in U.S. history, and the second largest oil spill in human history with over 800 million liters of hydrocarbons released into the Gulf of Mexico over a period of 3 months. Due to the widespread use of jet fuel hydrocarbons, this compound mixture has been recognized as the single largest chemical exposure for military personnel. Previous animal studies have demonstrated the ability of jet fuel (JP-8) exposure to promote the epigenetic transgenerational inheritance of disease susceptibility in subsequent generations. The diseases observed include late puberty, kidney, obesity and multiple disease pathologies. The current study is distinct and was designed to identify potential sperm DNA methylation biomarkers for specific transgenerational diseases. Observations show disease specific differential DNA methylation regions (DMRs) called epimutations in the transgenerational F3 generation great-grand-offspring male rats ancestrally exposed to jet fuel. The potential epigenetic DMR biomarkers were identified for late puberty, kidney, obesity, and multiple diseases, and found to be predominantly disease specific. These disease specific DMRs have associated genes that were previously shown to be linked with each of these specific diseases. Therefore, the germline (i.e. sperm) has environmentally induced ancestrally derived epimutations that have the potential to transgenerationally transmit disease susceptibilities to subsequent generations. Epigenetic biomarkers for specific diseases could be developed as medical diagnostics to facilitate clinical management of disease, and allow preventative medicine therapeutics.

***Correspondence**: Michael K. Skinner, Center for Reproductive Biology, School of Biological Sciences, Washington State University, Pullman, WA, 99164-4236, USA, Phone: 509-335-1524, skinner@wsu.edu.

Competing Interests

The authors declare no competing interests.

Declaration of interests

The authors declare that they have no known competing financial interests or personal relationships that could have appeared to influence the work reported in this paper.

Keywords

Epigenetics; Transgenerational; DNA Methylation; Jet Fuel; Puberty; Kidney; Obesity; Pathology

1. Introduction

Jet fuel is the generic name for hydrocarbon-based aviation fuels used in gas-turbine engine powered aircraft. Conventionally, jet fuel is obtained from the kerosene distillation fraction of crude oil, which is a complex blend of more than 1,000 different hydrocarbon chemical compounds. The main components are linear and branched alkanes and cycloalkanes. In the late 1930s, the first jet-powered aircrafts were developed, which involved two main operational standards of Jet A used in the US, and Jet A-1 used widely elsewhere in the world. The composition of hydrocarbon jet fuels has always been a compromise between the availability of suitable raw material, the requirement for processing, and performance for propulsion properties, safety, and engine-friendliness, but with no emphasis on the environmental impact [1].

A decade ago, the Deepwater Horizon oil rig explosion created the largest environmental disaster in U.S. history and the second largest oil spill in human history, with over 800 million liters of oil (hydrocarbons) released into the Gulf of Mexico over a period of 3 months [2]. According to data from the U.S. National Oceanic and Atmospheric Administration (NOAA), there were 137 oil spills in 2018, about 11 per month. Due to the widespread use of jet fuel JP-8, the military equivalent of Jet A-1 containing a corrosion inhibitor and anti-icing additive, this compound has been recognized as the single largest chemical exposure for U.S. and NATO military personnel [3]. Inhalation and dermal exposure have been shown to represent the primary routes of exposure [4].

Military and civilian personnel risk a widespread occupational exposure that can result in toxicity to the immune system, nervous system, and the respiratory tract [5]. Although various types of hydrocarbon exposures exist, such as automotive fuels and oil spills, the majority of the studies have focused on the direct exposure to JP-8 as a model hydrocarbon mixture. Human exposure to hydrocarbons have been linked to emotional dysfunction, decreased attention spans, fatigue, skin irritation, postural sway imbalances, and adverse effects on sensorimotor speed, liver function, and the respiratory system [6–10]. In animal studies, slight dermal irritation, weak dermal sensitization, respiratory tract sensory irritation, hearing loss, nephropathy, immunosuppressive and neurobehavioral effects have been correlated to exposure to JP-8 [11]. The no observable adverse effect level (NOAEL) for JP-8 is 500–1000 mg/kg BW/day [12]. Other adverse effects have been reported such as lung ventilatory function [6], immune dysfunction [13, 14], increased tumor formation [15] and suppressed immune response to viral infections [16].

During fetal gonadal development, exposure to various toxicants can be particularly detrimental. A study has shown that gestational exposure of rat dams to JP-8 leads to higher rates of renal disorders in offspring of both sexes, and higher incidence of reproductive insults such as prostate and pubertal abnormalities in males, primordial follicle loss and polycystic ovarian disease in females [17]. Analysis of the F3 generation great-grand-

offspring sperm detected 33 differential DNA methylation regions, termed epimutations [17]. The biological mechanism underlying this generational phenomenon is called epigenetic transgenerational inheritance [18]. Epigenetics is defined as molecular factors or processes around DNA that regulate genome activity, independent of DNA sequence, and are mitotically stable [19]. The epigenetic transgenerational inheritance is defined by the transmission of an altered epigenome and phenotypes through the germline in the absence of continued direct environmental exposures [18, 20].

In the rodent models, at around embryonic day E10-E12, the primordial germ cells undergo extensive epigenetic reprogramming, including a genome-wide reduction of 5-methylcytosine (5mC), to become stem-like cells for the germline [21]. A re-methylation occurs upon gonadal sex determination in a sex specific manner to generate the sperm or egg [22]. Environmental insults during this developmental period can alter the epigenetic reprogramming, and the altered DNA methylation patterns appear to become permanently programmed, similarly to the DNA methylation of an imprinted gene [19, 23]. These epigenetic changes are transmitted from the germline to the zygote and then to the embryonic stem cells, which will result in an altered epigenome and transcriptome in all somatic cells in future generations [19]. Ancestral exposure to environmental influences such as toxicants, abnormal nutrition, and traumatic stress can affect the germline epigenome and promote the epigenetic transgenerational inheritance of adult onset disease in various organisms from plants to humans [19]. Therefore, a need exists to identify predictive epigenetic biomarkers of environmental insult due to exposure to chemical toxicants. These epimutations (DNA methylation, histone modifications, non-coding RNA, chromatin structure, and RNA methylation alterations) could be used as biomarkers of exposure and disease [24]. The pesticide DDT [25, 26], the herbicide atrazine [27], and the agricultural fungicide vinclozolin [28, 29] have been shown to promote transgenerational epimutations associated with disease as potential pathology biomarkers.

The current study utilizes an epigenome-wide association study (EWAS) to identify DMRs associated with specific transgenerational diseases. Although our previous study demonstrated jet fuel was able to promote transgenerational sperm epimutations and various diseases [17], the current study is distinct and is designed to identify potential transgenerational epigenetic biomarkers in sperm for specific male diseases. Although transgenerational female disease has been observed, insufficient oocyte numbers prevent such analysis in females. The biological mechanisms underlying transgenerational epigenetic inheritance induced by jet fuel exposure are further investigated in the current study. An epigenome-wide association study (EWAS) compares individual males within the jet fuel lineage with a specific disease or pathology to those without any disease in order to identify epigenetic biomarkers for disease.

2. Methods

2.1 Animal studies and breeding

As previously described [17], female and male rats of an outbred strain Hsd:Sprague Dawley SD (Harlan) were fed *ad lib* with a standard rat diet and ad lib tap water. Timed-pregnant females (n=5) at 70 to 100 days of age were mated and on days 8 through 14 of gestation

[30] were administered daily intraperitoneal injections of JP-8 hydrocarbon (jet fuel obtained from Lt Dean Wagner, Dayton, OH), 500 mg/kg/BW/day, or dimethyl sulfoxide (DMSO) with an equal volume of sesame oil (Sigma) to prevent irritation at the injection site.

The gestating female rats treated were designated as the F0 generation. F1–F3 generation control and jet fuel lineages were housed in the same room and racks with lighting, food and water as previously described [20, 24, 30]. Non-littermate females and males aged 70–100 days from F1 generation of jet fuel or control lineages were bred to others within their treatment group obtain F2 generation offspring. Un-related F2 generation rats were bred to obtain F3 generation offspring. Only the F0 generation received treatments and they exhibited no gross pathology upon dissection. Onset of puberty was assessed in males starting at 35 days of age by the presence of balanopreputial separation. All experimental protocols for the procedures with rats were pre-approved by the Washington State University Animal Care and Use Committee (IACUC approval # 2568). All methods were performed in accordance with the relevant guidelines and regulations. The sperm samples from the previous study [17] were archived and used for the current study.

The current study was designed to investigate transgenerational F3 generation pathology and epimutation associations in sperm. Therefore, the F1 and F2 generation direct exposures were not investigated. The male transgenerational disease was assessed and correlated to sperm epimutations. Although females develop transgenerational disease, insufficient numbers of oocytes can be obtained on individuals to allow epigenetic associations to be assessed. Therefore, the study only examined male pathology and associated sperm epimutation associations.

2.2 Tissue harvest and histology processing

As previously described [17], at 12 months of age, rats were euthanized by CO_2 inhalation and cervical dislocation for tissue harvest. Testis, prostate, ovary, and kidney, were fixed in Bouin's solution (Sigma) followed by 70% ethanol, then processed for paraffin embedding and hematoxylin, and eosin (H & E) staining by standard procedures for histopathological examination. Paraffin five microns sections were processed, stained, and processed by Nationwide Histology, Spokane WA, USA. The current study used archived frozen sperm at −80C and slides and paraffin blocks from the previous study [17]. Previous studies have shown that slides and paraffin blocks, as well as frozen sperm, are stable for decades [31, 32].

2.3 Histopathology examination and disease classification

Archived histology slides or paraffin blocks from the previous study were used for a new histology analysis for the current study. Stained testis, prostate, and kidney slides were imaged through a microscope using 4x objective lenses (testis and prostate) or 10x objective lenses (kidney). Tiled images were captured using a digital camera. Tiled images for each tissue were photo-merged into a single image using Adobe Photoshop (ver. 21.1.2, Adobe, Inc.). Images were evaluated and pathology features digitally marked using Photoshop software. The Washington Animal Disease Diagnostic Laboratory (WADDL) at the

Washington State University College of Veterinary Medicine has board certified veterinary pathologists, and assisted in initially establishing the criteria for the pathology analyses and identifying parameters to assess [33]. The tissues evaluated histologically were selected from previous literature showing them to have pathology in transgenerational models [18, 23, 26, 27, 33–37], with an emphasis on reproductive organs. Histopathology readers were trained to recognize the specific abnormalities evaluated for this study in rat testis, ventral prostate, and kidney. Two individuals blinded to the exposure evaluated each tissue image for abnormalities. If there was disagreement about the disease status, then a third individual blinded to the exposure evaluated the tissue. A set of quality control (QC) slides were generated for each tissue, and were read by each reader prior to evaluating any set of experimental slides. These QC slide results were monitored for reader accuracy and concordance.

As previously described [19], testis histopathology criteria included the presence of vacuoles in the seminiferous tubules, azoospermic atretic seminiferous tubules, and ‘other’ abnormalities including sloughed spermatogenic cells in center of the tubule and a lack of a tubule lumen. As previously described [38, 39], prostate histopathology criteria included the presence of vacuoles in the glandular epithelium, atrophic glandular epithelium and hyperplasia of prostatic gland epithelium. Kidney histopathology criteria included reduced size of glomerulus, thickened Bowman’s capsule, and the presence of proteinaceous fluid-filled cysts > 50μm in diameter. A cutoff was established to declare a tissue ‘diseased’ based on the mean number of histopathological abnormalities plus two standard deviations from the mean of control group tissues, as assessed by each of the three individual observers blinded to the treatment groups. This number (i.e. greater than two standard deviations) was used to classify rats into those with and without testis, prostate, or kidney disease in each lineage. A rat tissue section was finally declared ‘diseased’ only when at least two of the three observers marked the same tissue section ‘diseased’. Obesity was assessed with an increase in body mass and a qualitative evaluation of abdominal adiposity, as previously described [26, 34, 40–42]. The statistical analyses for pathology results were expressed as the proportion of affected animals that exceeded a pre-determined threshold (testis, prostate, or kidney disease frequency, tumor frequency, obese frequency). Groups were analyzed using Fisher’s exact test. The pathologies and histological images were similar to those previously reported.

2.4 Epididymal sperm collection and DNA isolation

The protocol is described in detail in reference [17]. Briefly, the epididymis was dissected free of fat and connective tissue, then, after cutting open the cauda, placed into 6 ml of phosphate buffer saline (PBS) for 20 minutes at room temperature. Further incubation at 4°C will immobilize the sperm. The tissue was then minced, the released sperm was pelleted at 4°C 3,000 x *g* for 10 minutes, then resuspended in NIM buffer and stored at −80°C for further processing. An appropriate amount of rat sperm suspension was used for DNA extraction. Previous studies have shown mammalian sperm heads are resistant to sonication unlike somatic cells [43, 44]. Somatic cells and debris were therefore removed by brief sonication (Fisher Sonic Dismembrator, model 300, power 25), then centrifugation and washing 1–2 times in 1X PBS. The resulting pellet was resuspended in 820 μl DNA

extraction buffer and 80 μl 0.1M DTT added, then incubated at 65°C for 15 minutes. 80 μl proteinase K (20 mg/ml) was added and the sample was incubated at 55°C for 2–3 hours under constant rotation. Protein was removed by addition of protein precipitation solution (300 μl, Promega A795A), incubation for 15 minutes on ice, then centrifugation at 13,500 rpm for 30 minutes at 4°C. One ml of the supernatant was precipitated with 2 μl of GlycoBlue (Invitrogen, AM9516) and 1 ml of cold 100 % isopropanol. After incubation, the sample was spun at 13,500 x *g* for 30 min at 4°C, then washed with 70% cold ethanol. The pellet was air-dried for about 5 minutes then resuspended in 100 μl of nuclease free water.

2.5 Methylated DNA Immunoprecipitation (MeDIP)

The archived sperm samples were prepped as previously described [17]. Genomic DNA was sonicated and run on 1.5% agarose gel for fragment size verification. The sonicated DNA was then diluted with 1X TE buffer to 400 μl, then heat-denatured for 10 minutes at 95°C, and immediately cooled on ice for 10 minutes to create single-stranded DNA fragments. Then 100 μl of 5X IP buffer and 5 μg of antibody (monoclonal mouse anti 5-methyl cytidine; Diagenode #C15200006) were added, and the mixture was incubated overnight on a rotator at 4°C. The following day magnetic beads (Dynabeads M280 Sheep anti-Mouse IgG; Life Technologies 11201D) were pre-washed per manufacturer's instructions, and 50 μl of beads were added to the 500 μl of DNA-antibody mixture from the overnight incubation, then incubated for 2 hours on a rotator at 4°C. After this incubation, the samples were washed three times with 1X IP buffer using a magnetic rack. The washed samples were then resuspended in 250 μl digestion buffer (5mM Tris PH 8, 10.mM EDTA, 0.5% SDS) with 3.5 μl Proteinase K (20 mg/ml), and incubated for 2–3 hours on a rotator at 55°C. DNA clean-up was performed using a Phenol-Chloroform-Isoamyl-Alcohol extraction, and the supernatant precipitated with 2 μl of GlycoBlue (20 mg/ml), 20 μl of 5M NaCl and 500 μl ethanol in −20°C freezer for one to several hours. The DNA precipitate was pelleted, washed with 70% ethanol, then dried and resuspended in 20 μl H_2O or 1X TE. DNA concentration was measured in Qubit (Life Technologies) with the ssDNA kit (Molecular Probes Q10212).

2.6 MeDIP-Seq Analysis

As previously described [45], MeDIP DNA was used to create libraries for next generation sequencing (NGS) using the NEBNext Ultra RNA Library Prep Kit for Illumina (San Diego, CA) starting at step 1.4 of the manufacturer's protocol to generate double stranded DNA from the single-stranded DNA resulting from MeDIP. After this step, the manufacturer's protocol was followed indexing each sample individually with NEBNext Multiplex Oligos for Illumina. The WSU Spokane Genomics Core sequenced the samples on the Illumina HiSeq 2500 at PE50, with a read size of approximately 50 bp and approximately 20 million reads per pool. Eleven libraries were run in one lane.

2.7 Statistics and Bioinformatics

The DMR identification and annotation methods follow those presented in previous published papers [27, 45]. Data quality was assessed using the FastQC program (https://www.bioinformatics.babraham.ac.uk/projects/fastqc/), and reads were cleaned and filtered to remove adapters and low quality bases using Trimmomatic [46]. The reads for each MeDIP sample were mapped to the Rnor 6.0 rat genome using Bowtie2 [47] with default parameter

options. The mapped read files were then converted to sorted BAM files using SAMtools [48]. The MEDIPS R package [49] was used to calculate differential coverage between control and exposure sample groups. The edgeR p-value [50] was used to determine the relative difference between the two groups for each genomic window. Windows with an edgeR p-value less than an arbitrarily selected threshold were considered DMR. The site edges were extended until no genomic window with an edgeR p-value less than 0.1 remained within 1000 bp of the DMR. The edgeR p-value was used to assess the significance of the DMR identified. Due in part to the lower number of individuals with one specific disease type, a false discovery rate (FDR) analysis was not useful with the majority of the edgeR p<1e-04 having an FDR p>0.1. The low sample number for FDR and permutation analysis is a limitation to the current study [51–56]. Differential epimutation sites were annotated using the biomaRt R package [57] to access the Ensembl database [58]. The DMR associated genes were then automatically sorted into functional groups using information provided by the DAVID [59] and Panther [60] databases incorporated into an internal curated database (www.skinner.wsu.edu under genomic data). A Pathway Studio, Elsevier, database and network tool was used to assess physiological and disease process gene correlations. All molecular data has been deposited into the public database at NCBI (GEO # GSE155922) and R code computational tools available at GitHub (https://github.com/skinnerlab/MeDIP-seq) and www.skinner.wsu.edu.

3. Results

3.1 Animal Breeding

As previously described, from embryonic day E8 to E14 the F0 generation gestating females were administered daily intraperitoneal injections of JP-8 hydrocarbon (jet fuel obtained from Lt Dean Wagner, Dayton, OH), 500 mg/kg BW/day, or dimethyl sulfoxide (DMSO) (vehicle) with an equal volume of sesame oil (Sigma) to prevent irritation at the injection site [17]. The no observable adverse effect level (NOAEL) for JP-8 is 500–1000 mg/kg BW/day [12]. The offspring F1, F2 and F3 generations were all aged to 90 days of age and bred within the generation and within the jet fuel lineage. The F3 generation is the first without a direct exposure to jet fuel, and is thus called the transgenerational generation. All the animals were aged to 1 year and euthanized for pathology, and the sperm collected for epigenetic analyses. No sibling or cousin breeding was used to prevent any inbreeding artifacts in the control or jet fuel lineages. All protocols and studies were approved by the Washington State University Animal Care and Use Committee (IACUC approval # 2568).

3.2 Pathology Analysis

Archived histology slides from the previous study [17] were reanalyzed using a more advanced digital pathology procedure. Pathology analysis was performed by analyzing histology sections of prostate, testis, and kidney. Three different observers blinded to the exposure assessed the complete digitally acquired histological sections. The pathology parameters were identified, as previously described in the Methods section [25, 27, 28, 61]. Insufficient numbers of individuals with a single pathology were observed in order to perform an analysis for testis and prostate disease, Table 1. For the kidney pathology, the renal cysts, thickening of the Bowman’s capsule, and reduced glomerular size were

quantified. An increase in body mass index (BMI) and abdominal adiposity were assessed for obesity. For all the tissues, the number of abnormalities in an animal's tissue was compared with the mean number of abnormalities in the control group, which was significantly less than jet fuel lineage group, as previously described [17], Supplemental Table S1, to determine if that tissue was diseased, as described in the Methods. Age of puberty was determined by the day of preputial separation at the penis, as previously described [27]. For the F3 generation jet fuel lineage male pathology, the individual animals are listed with a (+) indicating presence of disease / pathology and a (−) indicating the absence of disease / pathology (Table 1). For any specific pathology, individuals were only selected for analysis if they had that single pathology. Animals with multiple disease (≥2) were identified and grouped for a multiple disease analysis. A more accurate association with the epimutations is possible with this strategy, and it eliminates the confounding presence of other disease. The jet fuel induced transgenerational diseases / pathologies that had sufficient numbers of animals were late puberty (4 males), kidney disease (5 males), obesity (6 males), and multiple disease (4 males), Table 1. Those individuals with a single disease were used to investigate the sperm disease associated DMRs (i.e. epigenetic biomarkers).

3.3 Sperm DNA methylation analysis

The sperm samples collected and maintained at −80 °C from the previous study [17] were used in an EWAS analysis to reanalyze the epigenetics with MeDIP-Seq technology on individual animals with a specific disease. The sperm samples were collected from the jet fuel lineage F3 generation individual males for epigenetic analysis. Within the jet fuel lineage, individual males with no disease were compared to individuals with a single specific disease (kidney, obesity, late puberty or multiple disease) in order to determine the disease specific differential DNA methylation regions (DMRs) (Figure 1A–D). By applying this strategy, the confounding effects of multiple disease are eliminated, and specific disease associated DMR biomarkers can be identified.

The sperm samples were collected, then the DNA was extracted, fragmented and the methylated DNA immunoprecipitated (MeDIP) using a methyl-cytosine antibody [45, 62]. An MeDIP-Seq analysis was performed on the methylated DNA fragments, as described in the Methods section [23, 45, 62]. The advantage to this procedure is that the majority of the epigenome is investigated (>90%) compared to other procedures biased to higher density CpG [63], and to the previously used tiling array procedure [17]. The DMR numbers are shown in Figure 1 with different edgeR statistical p-value cutoff thresholds, and the p<1e-04 (diseased versus non-diseased) was selected as the threshold for all subsequent analyses. The total number of DMRs (All Windows), if present, for each disease and multiple neighboring 1000 bp windows are presented (Figure 1). In our previous study, the MeDIP analysis used three pools of different animals to study the sperm DNA epimutations induced by the jet fuel treatment [17]. In the present study, individual animals were used to determine the transgenerational F3 generation jet fuel induced disease sperm DMR epimutations with MeDIP-Seq. For the p<1e-04, 280 DMRs were identified for the animals diagnosed with late puberty, with 125 DMRs (45%) having an increase in methylation (Figure 1A). The animals with kidney disease had 174 DMRs, with 77 DMRs (44%) having an increase in methylation

(Figure 1B). The animals with obesity had 174 DMRs with 70 DMRs (40%) having an increase in DNA methylation (Figure 1C). The animals with multiple disease had 463 DMRs identified with 217 DMRs (47%) having an increase in DNA methylation (Figure 1D). The disease specific DMRs with an edgeR p<1e-04 threshold are presented in Supplemental Tables S2–S5, with the log-fold-change (LFC) with a positive value indicating an increase in DNA methylation.

The disease specific DMR chromosomal locations are presented in Figure 2 where the red arrowheads represent the DMR locations, and the black boxes the DMR clusters. The late puberty, kidney, obesity and multiple disease analysis did not find any DMRs on the mitochondrial DNA (MT). Therefore, the DMRs were found on nearly all chromosomes. The DMRs length and their CpG density are presented in Figure 3. Between 1 and 4 CpG per 100 bp were found to be predominant, which is a characteristic of a low density CpG desert. This is similar to previously reported transgenerational DMRs [64]. The DMRs length for each disease DMR biomarker were 1–4 kb with 1 kb being predominant, Figure 3. Commonly, the DMRs are 1 kb in size with around 10 CpGs as previously reported [64]. For the different disease versus non-disease comparisons (late puberty biomarker, kidney disease biomarker, obesity disease biomarker, and multiple disease biomarker), a principal component analysis (PCA) shows a clustered separation of the late puberty, kidney, obesity, and multiple disease DMR components for read depth at DMR sites (Figure 4). The DMR PCA analysis was performed in part to identify any outlier samples, of which none were found. Therefore, the principal components of the pathology associated DMRs are distinct from the non-disease group for each of the pathologies.

An overlap of disease specific DMRs used a Venn diagram for chromosomal location overlaps at the p<1e-04 threshold to identify overlapping DMRs for each disease (late puberty, kidney, and multiple disease). The different diseases had unique DMRs with negligible overlap in the F3 generation sperm at a p<1e-04 (Figure 5A). To further study how the disease specific DMRs overlap, an extended overlap of the p<1e-04 DMRs was investigated. The DMRs with p<1e-04 were compared to DMRs with p<0.05 statistical threshold to allow for an increased potential to identify overlaps when a less stringent p-value was used. Between 9.6% and 17.9% overlap was found for each individual comparison, Figure 5B. Results indicate that the DMRs identified are primarily specific to one pathology. A final analysis determined the disease DMRs at p<0.05 and examined the overlap for all the pathologies, Figure 5C. As expected, the total numbers of DMRs dramatically increased. An overlap with 57 DMRs was observed for all the pathologies compared. A final Venn diagram overlap used the p<1e-04 DMRs for each of the pathologies with the p<0.05 overlapping 57 DMRs, Figure 5D. No overlapping DMR between the different pathology was observed, but some were observed with individual disease comparisons. Therefore, the different pathologies had predominantly unique DMRs with negligible overlaps.

3.4 DMR Gene Associations

For each disease specific DMR data sets, the gene associations were identified. In order to include the promoters, the DMRs with a gene within 10 kb distance were taken into account

as well as the associated genes and gene functional categories (Supplemental Tables S1–S4). The DMRs with a p<1e-04 were used for this analysis on the different diseases. Several predominant gene categories were identified such as signaling, metabolism, transcription, receptor and cytoskeleton for all the different disease DMR signatures, Figure 6A. Similar gene categories were observed for all the pathologies. A cellular KEGG pathway analysis was conducted to identify pathways that include the associated genes for each DMR data set, as described in the Methods. The top five pathways with DMR associated genes, listed in bracket, are presented in Figure 6B. The cellular pathways identified also had signaling and critical cellular processes involved.

Potential jet fuel transgenerational disease specific DMR associated genes were investigated for genes previously shown to associate with the specific diseases, Figures 7 and 8. The late puberty DMR biomarkers had strong correlations with genes linked to delayed or precocious puberty (Figure 7A). The kidney associated genes had strong correlations with genes associated with kidney disease, chronic renal failure, and polycystic kidney disease (Figure 7B). The obesity associated genes had strong correlations with genes involved in type 2 diabetes, obesity, insulin resistance, glomerulosclerosis, and metabolic syndrome (Figure 7C). The multiple disease DMR biomarkers had strong correlations with genes linked to kidney, kidney disease, cancer, prostate cancer, insulin resistance, and obesity (Figure 8). Interestingly, the multiple disease had components of each of the individual diseases observed, Figure 8. Observations that the disease specific DMR biomarker associated genes corelated with previously identified disease associated genes helps validate the DMR biomarkers identified.

4. Discussion

Hydrocarbon jet fuels are composed of long and short-chain aromatic and aliphatic hydrocarbons [65] and are found in jet propulsion fuels such as JP-4, JP-5, JP-7, JP-8, gasoline, diesel fuels and kerosene [66]. They are among the most common occupational chemical exposures encountered by military and civilian workers [67]. Acute toxicity following high levels of exposure to raw fuel products, fuel vapor or aerosol, or products of fuel combustion has been previously described in both animals and humans [3, 10, 68]. Each year, thousands of man-made substances are released into our environment. However, prospective risk assessment studies of these potentially harmful chemicals on human health are not required by current regulations [69]. In the North Atlantic Treaty Organization (NATO) countries, JP-8 is the most standard jet fuel utilized for military purposes. Every year, about 6 billion gallons of JP-8 are used [68]. JP-8, albeit less toxic and safer than JP-4, contains many ototoxic aromatic hydrocarbons [70]. Environmental exposure to jet fuels has been associated with several health conditions, such as immune system dysfunction, neurobehavioural problems, developmental/reproductive dysfunction and hepatic, pulmonary, renal and vestibular dysfunction [11, 68, 71, 72].

The current study evaluated the association between diseases resulting from ancestral exposure to jet fuel (JP-8) and the epigenetic alterations in sperm associated with these male pathologies. In our previous study, jet fuel exposure has been linked to the induction of transgenerational epigenetic modifications in rats [17]. Therefore, the previous study is

distinct from the current study objectives and experimental design. The histopathology slides and stored sperm samples from this previous study were reanalyzed with more advanced technology in the current study. Previously, paraffin blocks, as well as frozen sperm DNA methylation, have been shown to be stable for decades or longer [31, 32]. The observations in the present study found DNA methylation alterations associated with specific diseases in rats ancestrally exposed to jet fuel. The pathologies identified for analysis were late puberty, kidney disease, obesity, and multiple disease. Kidney disease is particularly relevant to human populations since it is one of the major causes of disease and mortality among men [73]. In addition, according to the Centers of Disease Control (CDC), in 2017–2018, the prevalence of obesity in the USA was 42.4 million people [74]. The current study used individual animals with only one specific disease or pathology identified. This reduces the confounding effects of the presence of other pathologies. Therefore, the disease epigenetic signature identified reflects the specific disease, but this limited the number of individuals investigated.

Genome-wide association studies (GWAS) have found specific genetic mutations associated with human pathologies, however these genetic mutations generally appear in less than 1% of the disease population [75, 76]. In contrast, epimutations seem to have a higher frequency and appear in more individuals with the diseases [27, 28, 77]. Therefore, determining epigenetic biomarkers for these diseases could become especially useful indicators of environmental exposures and disease susceptibility in the human population [77]. The current study supports this concept and demonstrates disease specific epimutations can be identified. One of the main objectives was to determine if a common set of DMRs may exist between different diseases to suggest a molecular cause for increased disease susceptibility.

Observations show that the number of differential methylated regions (DMRs) found in the transgenerational F3 males is between 100 and 500 at an edgeR $p<1e-04$ threshold (Figure 1) for each individual pathology. Few DMRs overlap between the different pathologies which supports the possible use of epimutations as biomarkers of disease. Although further studies are required, the lack of a subpopulation of DMRs overlapping with all pathologies suggests that at a more stringent statistical threshold there are not common DMRs among specific diseases. Interestingly, there are predominantly disease specific DMRs promoting a specific disease. The DMR associated genes indicate that signaling, metabolism, transcription, receptor, cytoskeleton and development were the most affected gene categories. The identification of previously identified disease specific linked genes in the DMR associated genes helps validate the observations made.

A limitation of the current study was the low numbers of animals available with a specific individual disease. Although an edgeR p-value was used to identify and analyze the disease associated DMRs, further analyses adjusting for multiple testing using the false discovery rate (FDR) resulted in FDR p-values for the disease epimutations of >0.1 in all comparisons except the multiple disease phenotype, which retained 67 DMRs at an FDR $p<0.1$. The low sample number is likely the most important limitation in the current analysis. Potential higher variability in the data needs to be considered even though higher edgeR values were used, but this does not address multiple testing corrections. Future studies will need to use

higher n-values and/or better statistical models to reduce this FDR analysis limitation [51–56].

Observations suggest that jet fuel induced transgenerational DMRs present in sperm are associated with specific diseases. The identification of these epigenetic biomarkers could potentially be used to assess transgenerational transmission of various pathology susceptibilities in future generation offspring. Consequently, such epigenetic biomarkers could be utilized or developed as potential diagnostics and potentially facilitate preventative therapeutics. Although more extensive studies in humans are required, the present study helps support the proof of concept that associated pathology DMRs could be used as epigenetic biomarkers. The potential use of disease DMR biomarkers as early disease susceptibility diagnostics, prior to the actual onset of diseases, will allow preventative therapeutics or clinical management of disease to be considered.

The current study used an EWAS approach to examine jet fuel induction of transgenerational diseases. Observations provide evidence that environmental and disease specific biomarkers can be identified and potentially be used as a diagnostic tool for disease susceptibility in the future. Since epigenetic biomarkers appear to have a high frequency of association with pathologies, their incorporation in clinical medicine could facilitate preventative medicine.

Supplementary Material

Refer to Web version on PubMed Central for supplementary material.

Acknowledgments

We acknowledge Ms. Michelle Pappalardo, Mr. Ryan Thompson, Ms. Skylar Shea Davidson, Ms. Makena Horne, Ms. Emma Impala, and Ms. Rachel LaRosa for technical assistance. We acknowledge Ms. Amanda Quilty for editing and Ms. Heather Johnson for assistance in preparation of the manuscript. We thank the Genomics Core laboratory at WSU Spokane for sequencing data. This study was supported by John Templeton Foundation (50183 and 61174) (https://templeton.org/) grants to MKS and NIH (ES012974) (https://www.nih.gov/) grant to MKS. The funders had no role in study design, data collection and analysis, decision to publish, or preparation of the manuscript.

Abbreviations

JP-8	jet fuel
DMRs	DNA methylation regions
NOAA	National Oceanic and Atmospheric Administration
5mC	5-methylcytosine
EWAS	epigenome-wide association study
DMSO	dimethyl sulfoxide
BMI	body mass index
MeDIP	methylated DNA immunoprecipitated

LFC	log-fold-change
PCA	principal component analysis
NATO	North Atlantic Treaty Organization
CDC	Centers of Disease Control
GWAS	Genome-wide association studies
FDR	false discovery rate
WADDL	Washington Animal Disease Diagnostic Laboratory
QC	quality control
BMI	body mass index
PBS	phosphate buffer saline
NGS	next generation sequencing

References

[1]. Kallio P, Pasztor A, Akhtar MK, and Jones PR, Renewable jet fuel. Curr Opin Biotechnol, 2014 26: p. 50–5. [PubMed: 24679258]

[2]. Barron MG, Ecological impacts of the deepwater horizon oil spill: implications for immunotoxicity. Toxicol Pathol, 2012 40(2): p. 315–20. [PubMed: 22105647]

[3]. Carlton GN and Smith LB, Exposures to jet fuel and benzene during aircraft fuel tank repair in the U.S. Air Force. Appl Occup Environ Hyg, 2000 15(6): p. 485–91. [PubMed: 10853289]

[4]. Chao YC, Gibson RL, and Nylander-French LA, Dermal exposure to jet fuel (JP-8) in US Air Force personnel. Ann Occup Hyg, 2005 49(7): p. 639–45. [PubMed: 16006502]

[5]. National Research Council (US), S.o.J.-P.F., Toxicologic Assessment of Jet-Propulsion Fuel 8 Toxicologic Assessment of Jet-Propulsion Fuel 8. 2003, Washington (DC): National Academies Press (US).

[6]. Wong SS, Vargas J, Thomas A, Fastje C, McLaughlin M, Camponovo R, Lantz RC, Heys J, and Witten ML, In vivo comparison of epithelial responses for S-8 versus JP-8 jet fuels below permissible exposure limit. Toxicology, 2008 254(1–2): p. 106–11. [PubMed: 18930109]

[7]. Cohen GM, Pulmonary metabolism of foreign compounds: its role in metabolic activation. Environ Health Perspect, 1990 85: p. 31–41. [PubMed: 2200668]

[8]. Davies NE, Jet Fuel Intoxication. Aerosp Med, 1964 35: p. 481–2. [PubMed: 14170936]

[9]. Dossing M, Loft S, and Schroeder E, Jet fuel and liver function. Scand J Work Environ Health, 1985 11(6): p. 433–7. [PubMed: 4095521]

[10]. Smith LB, Bhattacharya A, Lemasters G, Succop P, Puhala E 2nd, Medvedovic M, and Joyce J, Effect of chronic low-level exposure to jet fuel on postural balance of US Air Force personnel. J Occup Environ Med, 1997 39(7): p. 623–32. [PubMed: 9253723]

[11]. Mattie DR and Sterner TR, Past, present and emerging toxicity issues for jet fuel. Toxicol Appl Pharmacol, 2011 254(2): p. 127–32. [PubMed: 21296101]

[12]. Cooper JR and Mattie DR, Developmental toxicity of JP-8 jet fuel in the rat. J Appl Toxicol, 1996 16(3): p. 197–200. [PubMed: 8818858]

[13]. Harris DT, Sakiestewa D, Titone D, Robledo RF, Young RS, and Witten M, Jet fuel-induced immunotoxicity. Toxicol Ind Health, 2000 16(7–8): p. 261–5. [PubMed: 11693943]

[14]. Hilgaertner JW, He X, Camacho D, Badowski M, Witten M, and Harris DT, The influence of hydrocarbon composition and exposure conditions on jet fuel-induced immunotoxicity. Toxicol Ind Health, 2011 27(10): p. 887–98. [PubMed: 21402657]

[15]. Harris DT, Sakiestewa D, Titone D, He X, Hyde J, and Witten M, JP-8 jet fuel exposure potentiates tumor development in two experimental model systems. Toxicol Ind Health, 2007 23(10): p. 617–23. [PubMed: 18717520]

[16]. Harris DT, Sakiestewa D, Titone D, He X, Hyde J, and Witten M, JP-8 jet fuel exposure suppresses the immune response to viral infections. Toxicol Ind Health, 2008 24(4): p. 209–16. [PubMed: 19022873]

[17]. Tracey R, Manikkam M, Guerrero-Bosagna C, and Skinner M, Hydrocarbons (jet fuel JP-8) induce epigenetic transgenerational inheritance of obesity, reproductive disease and sperm epimutations. Reproductive Toxicology, 2013 36: p. 104–116. [PubMed: 23453003]

[18]. Anway MD, Cupp AS, Uzumcu M, and Skinner MK, Epigenetic transgenerational actions of endocrine disruptors and male fertility. Science, 2005 308(5727): p. 1466–9. [PubMed: 15933200]

[19]. Nilsson E, Sadler-Riggleman I, and Skinner MK, Environmentally Induced Epigenetic Transgenerational Inheritance of Disease. Environmental Epigenetics, 2018 4(2): p. 1–13, dvy016.

[20]. Skinner MK, Manikkam M, and Guerrero-Bosagna C, Epigenetic transgenerational actions of environmental factors in disease etiology. Trends Endocrinol Metab, 2010 21(4): p. 214–22. [PubMed: 20074974]

[21]. Hajkova P, Ancelin K, Waldmann T, Lacoste N, Lange UC, Cesari F, Lee C, Almouzni G, Schneider R, and Surani MA, Chromatin dynamics during epigenetic reprogramming in the mouse germ line. Nature, 2008 452(7189): p. 877–81. [PubMed: 18354397]

[22]. Reik W, Dean W, and Walter J, Epigenetic reprogramming in mammalian development. Science, 2001 293(5532): p. 1089–93. [PubMed: 11498579]

[23]. Guerrero-Bosagna C, Settles M, Lucker B, and Skinner M, Epigenetic transgenerational actions of vinclozolin on promoter regions of the sperm epigenome. Plos One, 2010 5(9): p. 1–17, e13100.

[24]. Manikkam M, Guerrero-Bosagna C, Tracey R, Haque MM, and Skinner MK, Transgenerational actions of environmental compounds on reproductive disease and identification of epigenetic biomarkers of ancestral exposures. PLoS ONE 2012 7(2): p. 1–12, e31901.

[25]. King SE, McBirney M, Beck D, Sadler-Riggleman I, Nilsson E, and Skinner MK, Sperm Epimutation Biomarkers of Obesity and Pathologies following DDT Induced Epigenetic Transgenerational Inheritance of Disease. Environ Epigenet, 2019 5(2): p. 1–15, dvz008.

[26]. Skinner MK, Manikkam M, Tracey R, Guerrero-Bosagna C, Haque MM, and Nilsson E, Ancestral dichlorodiphenyltrichloroethane (DDT) exposure promotes epigenetic transgenerational inheritance of obesity. BMC Medicine, 2013 11: p. 228, 1–16. [PubMed: 24228800]

[27]. McBirney M, King SE, Pappalardo M, Houser E, Unkefer M, Nilsson E, Sadler-Riggleman I, Beck D, Winchester P, and Skinner MK, Atrazine Induced Epigenetic Transgenerational Inheritance of Disease, Lean Phenotype and Sperm Epimutation Pathology Biomarkers. PLoS One, 2017 12(9): p. 1–37, e0184306.

[28]. Nilsson E, King SE, McBirney M, Kubsad D, Pappalardo M, Beck D, Sadler-Riggleman I, and Skinner MK, Vinclozolin induced epigenetic transgenerational inheritance of pathologies and sperm epimutation biomarkers for specific diseases. PLoS One, 2018 13(8): p. 1–29, e0202662.

[29]. Stouder C and Paoloni-Giacobino A, Transgenerational effects of the endocrine disruptor vinclozolin on the methylation pattern of imprinted genes in the mouse sperm. Reproduction, 2010 139(2): p. 373–9. [PubMed: 19887539]

[30]. Nilsson EE, Anway MD, Stanfield J, and Skinner MK, Transgenerational epigenetic effects of the endocrine disruptor vinclozolin on pregnancies and female adult onset disease. Reproduction, 2008 135(5): p. 713–21. [PubMed: 18304984]

[31]. Ono Y, Sato H, Miyazaki T, Fujiki K, Kume E, and Tanaka M, Quality assessment of long-term stored formalin-fixed paraffin embedded tissues for histopathological evaluation. J Toxicol Pathol, 2018 31(1): p. 61–64. [PubMed: 29479142]

[32]. Huang C, Lei L, Wu HL, Gan RX, Yuan XB, Fan LQ, and Zhu WB, Long-term cryostorage of semen in a human sperm bank does not affect clinical outcomes. Fertil Steril, 2019 112(4): p. 663–669 e1. [PubMed: 31371041]

[33]. Anway MD, Leathers C, and Skinner MK, Endocrine disruptor vinclozolin induced epigenetic transgenerational adult-onset disease. Endocrinology, 2006 147(12): p. 5515–23. [PubMed: 16973726]

[34]. Manikkam M, Tracey R, Guerrero-Bosagna C, and Skinner M, Pesticide and Insect Repellent Mixture (Permethrin and DEET) Induces Epigenetic Transgenerational Inheritance of Disease and Sperm Epimutations. Reproductive Toxicology 2012 34(4): p. 708–719. [PubMed: 22975477]

[35]. Manikkam M, Tracey R, Guerrero-Bosagna C, and Skinner M, Plastics Derived Endocrine Disruptors (BPA, DEHP and DBP) Induce Epigenetic Transgenerational Inheritance of Obesity, Reproductive Disease and Sperm Epimutations. PLoS ONE, 2013 8(1): p. 1–18, e55387.

[36]. Manikkam M, Tracey R, Guerrero-Bosagna C, and Skinner MK, Dioxin (TCDD) induces epigenetic transgenerational inheritance of adult onset disease and sperm epimutations. PLoS ONE, 2012 7(9): p. 1–15, e46249.

[37]. Manikkam M, Haque MM, Guerrero-Bosagna C, Nilsson E, and Skinner MK, Pesticide methoxychlor promotes the epigenetic transgenerational inheritance of adult onset disease through the female germline. PLoS ONE, 2014 9(7): p. 1–19, e102091.

[38]. Anway MD and Skinner MK, Transgenerational effects of the endocrine disruptor vinclozolin on the prostate transcriptome and adult onset disease. Prostate, 2008 68(5): p. 517–29. [PubMed: 18220299]

[39]. Taylor JA, Richter CA, Ruhlen RL, and vom Saal FS, Estrogenic environmental chemicals and drugs: mechanisms for effects on the developing male urogenital system. J Steroid Biochem Mol Biol, 2011 127(1–2): p. 83–95. [PubMed: 21827855]

[40]. McAllister EJ, Dhurandhar NV, Keith SW, Aronne LJ, Barger J, Baskin M, Benca RM, Biggio J, Boggiano MM, Eisenmann JC, Elobeid M, Fontaine KR, Gluckman P, Hanlon EC, Katzmarzyk P, Pietrobelli A, Redden DT, Ruden DM, Wang C, Waterland RA, Wright SM, and Allison DB, Ten putative contributors to the obesity epidemic. Critical Reviews in Food Science and Nutrition, 2009 49(10): p. 868–913. [PubMed: 19960394]

[41]. Xie F, Zhang R, Yang C, Xu Y, Wang N, Sun L, Liu J, Wei R, and Ai J, Long-term neuropeptide Y administration in the periphery induces abnormal baroreflex sensitivity and obesity in rats. Cell Physiol Biochem, 2012 29(1–2): p. 111–20. [PubMed: 22415080]

[42]. Phillips LK and Prins JB, The link between abdominal obesity and the metabolic syndrome. Curr Hypertens Rep, 2008 10(2): p. 156–64. [PubMed: 18474184]

[43]. Huang TT Jr. and Yanagimachi R, Inner acrosomal membrane of mammalian spermatozoa: its properties and possible functions in fertilization. Am J Anat, 1985 174(3): p. 249–68. [PubMed: 3840952]

[44]. Calvin HI, Isolation of subfractionation of mammalian sperm heads and tails. Methods Cell Biol, 1976 13: p. 85–104. [PubMed: 772365]

[45]. Ben Maamar M, Sadler-Riggleman I, Beck D, McBirney M, Nilsson E, Klukovich R, Xie Y, Tang C, Yan W, and Skinner MK, Alterations in sperm DNA methylation, non-coding RNA expression, and histone retention mediate vinclozolin-induced epigenetic transgenerational inheritance of disease. Environmental Epigenetics, 2018 4(2): p. 1–19, dvy010.

[46]. Bolger AM, Lohse M, and Usadel B, Trimmomatic: a flexible trimmer for Illumina sequence data. Bioinformatics, 2014 30(15): p. 2114–20. [PubMed: 24695404]

[47]. Langmead B and Salzberg SL, Fast gapped-read alignment with Bowtie 2. Nature Methods, 2012 9(4): p. 357–9. [PubMed: 22388286]

[48]. Li H, Handsaker B, Wysoker A, Fennell T, Ruan J, Homer N, Marth G, Abecasis G, Durbin R, and S. Genome Project Data Processing, The Sequence Alignment/Map format and SAMtools. Bioinformatics, 2009 25(16): p. 2078–9. [PubMed: 19505943]

[49]. Lienhard M, Grimm C, Morkel M, Herwig R, and Chavez L, MEDIPS: genome-wide differential coverage analysis of sequencing data derived from DNA enrichment experiments. Bioinformatics, 2014 30(2): p. 284–6. [PubMed: 24227674]

[50]. Robinson MD, McCarthy DJ, and Smyth GK, edgeR: a Bioconductor package for differential expression analysis of digital gene expression data. Bioinformatics, 2010 26(1): p. 139–40. [PubMed: 19910308]

[51]. Nilsson R, Bjorkegren J, and Tegner J, On reliable discovery of molecular signatures. BMC Bioinformatics, 2009 10: p. 38. [PubMed: 19178740]

[52]. Jung SH, Sample size and power calculation for molecular biology studies. Methods Mol Biol, 2010 620: p. 203–18. [PubMed: 20652505]

[53]. Bretz F, Landgrebe J, and Brunner E, Multiplicity issues in microarray experiments. Methods Inf Med, 2005 44(3): p. 431–7. [PubMed: 16113769]

[54]. Yang H and Churchill G, Estimating p-values in small microarray experiments. Bioinformatics, 2007 23(1): p. 38–43. [PubMed: 17077100]

[55]. Higdon R, van Belle G, and Kolker E, A note on the false discovery rate and inconsistent comparisons between experiments. Bioinformatics, 2008 24(10): p. 1225–8. [PubMed: 18424815]

[56]. Devlin B, Roeder K, and Wasserman L, Analysis of multilocus models of association. Genet Epidemiol, 2003 25(1): p. 36–47. [PubMed: 12813725]

[57]. Durinck S, Spellman PT, Birney E, and Huber W, Mapping identifiers for the integration of genomic datasets with the R/Bioconductor package biomaRt. Nature Protocols, 2009 4(8): p. 1184–91. [PubMed: 19617889]

[58]. Cunningham F, Amode MR, Barrell D, Beal K, Billis K, Brent S, Carvalho-Silva D, Clapham P, Coates G, Fitzgerald S, Gil L, Giron CG, Gordon L, Hourlier T, Hunt SE, Janacek SH, Johnson N, Juettemann T, Kahari AK, Keenan S, Martin FJ, Maurel T, McLaren W, Murphy DN, Nag R, Overduin B, Parker A, Patricio M, Perry E, Pignatelli M, Riat HS, Sheppard D, Taylor K, Thormann A, Vullo A, Wilder SP, Zadissa A, Aken BL, Birney E, Harrow J, Kinsella R, Muffato M, Ruffier M, Searle SM, Spudich G, Trevanion SJ, Yates A, Zerbino DR, and Flicek P, Ensembl 2015. Nucleic Acids Research, 2015 43(Database issue): p. D662–9. [PubMed: 25352552]

[59]. Huang da W, Sherman BT, and Lempicki RA, Systematic and integrative analysis of large gene lists using DAVID bioinformatics resources. Nature Protocols, 2009 4(1): p. 44–57. [PubMed: 19131956]

[60]. Mi H, Muruganujan A, Casagrande JT, and Thomas PD, Large-scale gene function analysis with the PANTHER classification system. Nature Protocols, 2013 8(8): p. 1551–66. [PubMed: 23868073]

[61]. Kubsad D, Nilsson EE, King SE, Sadler-Riggleman I, Beck D, and Skinner MK, Assessment of Glyphosate Induced Epigenetic Transgenerational Inheritance of Pathologies and Sperm Epimutations: Generational Toxicology. Scientific Reports, 2019 9(1): p. 6372. [PubMed: 31011160]

[62]. Skinner MK, Ben Maamar M, Sadler-Riggleman I, Beck D, Nilsson E, McBirney M, Klukovich R, Xie Y, Tang C, and Yan W, Alterations in sperm DNA methylation, non-coding RNA and histone retention associate with DDT-induced epigenetic transgenerational inheritance of disease. Epigenetics & Chromatin 2018 11(1): p. 8, 1–24. [PubMed: 29482626]

[63]. Nair SS, Coolen MW, Stirzaker C, Song JZ, Statham AL, Strbenac D, Robinson MD, and Clark SJ, Comparison of methyl-DNA immunoprecipitation (MeDIP) and methyl-CpG binding domain (MBD) protein capture for genome-wide DNA methylation analysis reveal CpG sequence coverage bias. Epigenetics, 2011 6(1): p. 34–44. [PubMed: 20818161]

[64]. Skinner MK and Guerrero-Bosagna C, Role of CpG Deserts in the Epigenetic Transgenerational Inheritance of Differential DNA Methylation Regions. BMC Genomics 2014 15(1): p. 692. [PubMed: 25142051]

[65]. Ritchie GD, Still KR, Alexander WK, Nordholm AF, Wilson CL, Rossi J 3rd, and Mattie DR, A review of the neurotoxicity risk of selected hydrocarbon fuels. J Toxicol Environ Health B Crit Rev, 2001 4(3): p. 223–312. [PubMed: 11503417]

[66]. Guthrie OW, Wong BA, McInturf SM, Reboulet JE, Ortiz PA, and Mattie DR, Inhalation of Hydrocarbon Jet Fuel Suppress Central Auditory Nervous System Function. J Toxicol Environ Health A, 2015 78(18): p. 1154–69. [PubMed: 26408153]

[67]. Heaton KJ, Maule AL, Smith KW, Rodrigues EG, McClean MD, and Proctor SP, JP8 exposure and neurocognitive performance among US Air Force personnel. Neurotoxicology, 2017 62: p. 170–180. [PubMed: 28687449]

[68]. Ritchie G, Still K, Rossi J 3rd, Bekkedal M, Bobb A, and Arfsten D, Biological and health effects of exposure to kerosene-based jet fuels and performance additives. J Toxicol Environ Health B Crit Rev, 2003 6(4): p. 357–451. [PubMed: 12775519]

[69]. Melnick R, Lucier G, Wolfe M, Hall R, Stancel G, Prins G, Gallo M, Reuhl K, Ho SM, Brown T, Moore J, Leakey J, Haseman J, and Kohn M, Summary of the National Toxicology Program's report of the endocrine disruptors low-dose peer review. Environ Health Perspect, 2002 110(4): p. 427–31. [PubMed: 11940462]

[70]. Kaufman LR, LeMasters GK, Olsen DM, and Succop P, Effects of concurrent noise and jet fuel exposure on hearing loss. J Occup Environ Med, 2005 47(3): p. 212–8. [PubMed: 15761316]

[71]. Fife TD, Robb MJA, Steenerson KK, and Saha KC, Bilateral Vestibular Dysfunction Associated With Chronic Exposure to Military Jet Propellant Type-Eight Jet Fuel. Front Neurol, 2018 9: p. 351. [PubMed: 29867750]

[72]. Long RJ and Charles RA, Aviation Fuel Exposure Resulting in Otitis Externa with Vertigo. Aerosp Med Hum Perform, 2018 89(7): p. 661–663. [PubMed: 29921359]

[73]. Hill NR, Fatoba ST, Oke JL, Hirst JA, O'Callaghan CA, Lasserson DS, and Hobbs FD, Global Prevalence of Chronic Kidney Disease - A Systematic Review and Meta-Analysis. PLoS One, 2016 11(7): p. e0158765. [PubMed: 27383068]

[74]. Hales CM, Carroll MD, Fryar CD, and Ogden CL, Prevalence of Obesity and severe obesity among adults: United States, 2017–2018. NCHS data brief, 2020(360): p. 1–8.

[75]. van der Ende MY, Said MA, van Veldhuisen DJ, Verweij N, and van der Harst P, Genome-wide studies of heart failure and endophenotypes: lessons learned and future directions. Cardiovasc Res, 2018 114(9): p. 1209–1225. [PubMed: 29912321]

[76]. Belizario JE, The humankind genome: from genetic diversity to the origin of human diseases. Genome, 2013 56(12): p. 705–16. [PubMed: 24433206]

[77]. Flanagan JM, Epigenome-wide association studies (EWAS): past, present, and future. Methods Mol Biol, 2015 1238: p. 51–63. [PubMed: 25421654]

Highlights

- Jet fuel hydrocarbons promote epigenetic transgenerational inheritance of disease.
- Sperm epimutation biomarkers identified for transgenerational puberty, kidney, obesity disease.
- Disease specific epigenetic biomarkers identified with negligible overlap.

A Late Puberty DMR Biomarkers

p-value	All Window	Multiple Window
0.001	1701	3
1e-04	**280**	**0**
1e-05	47	0
1e-06	12	0
1e-07	1	0
Significant windows		1
Number of DMR		280

B Kidney Disease DMR Biomarkers

p-value	All Window	Multiple Window
0.001	1254	3
1e-04	**174**	**0**
1e-05	25	0
1e-06	5	0
1e-07	1	0
Significant windows		1
Number of DMR		174

C Obesity Disease DMR Biomarkers

p-value	All Window	Multiple Window
0.001	1208	1
1e-04	**174**	**0**
1e-05	25	0
1e-06	3	0
1e-07	0	0
Significant windows		1
Number of DMR		174

D Multiple Disease DMR Biomarkers

p-value	All Window	Multiple Window
0.001	2841	18
1e-04	**463**	**0**
1e-05	88	0
1e-06	18	0
1e-07	4	0
Significant windows		1
Number of DMR		463

Figure 1.

DMR identification and numbers. The number of DMRs found using different p-value cutoff thresholds. The All Window column shows all DMRs. The Multiple Window column shows the number of DMRs containing at least two significant windows (1 kb each). The number of DMRs with the number of significant windows (1 kb per window) at a p-value threshold bolded for DMR. **(A)** Late puberty DMRs; **(B)** Kidney disease DMRs; **(C)** Obesity disease DMRs; and **(D)** Multiple disease DMRs.

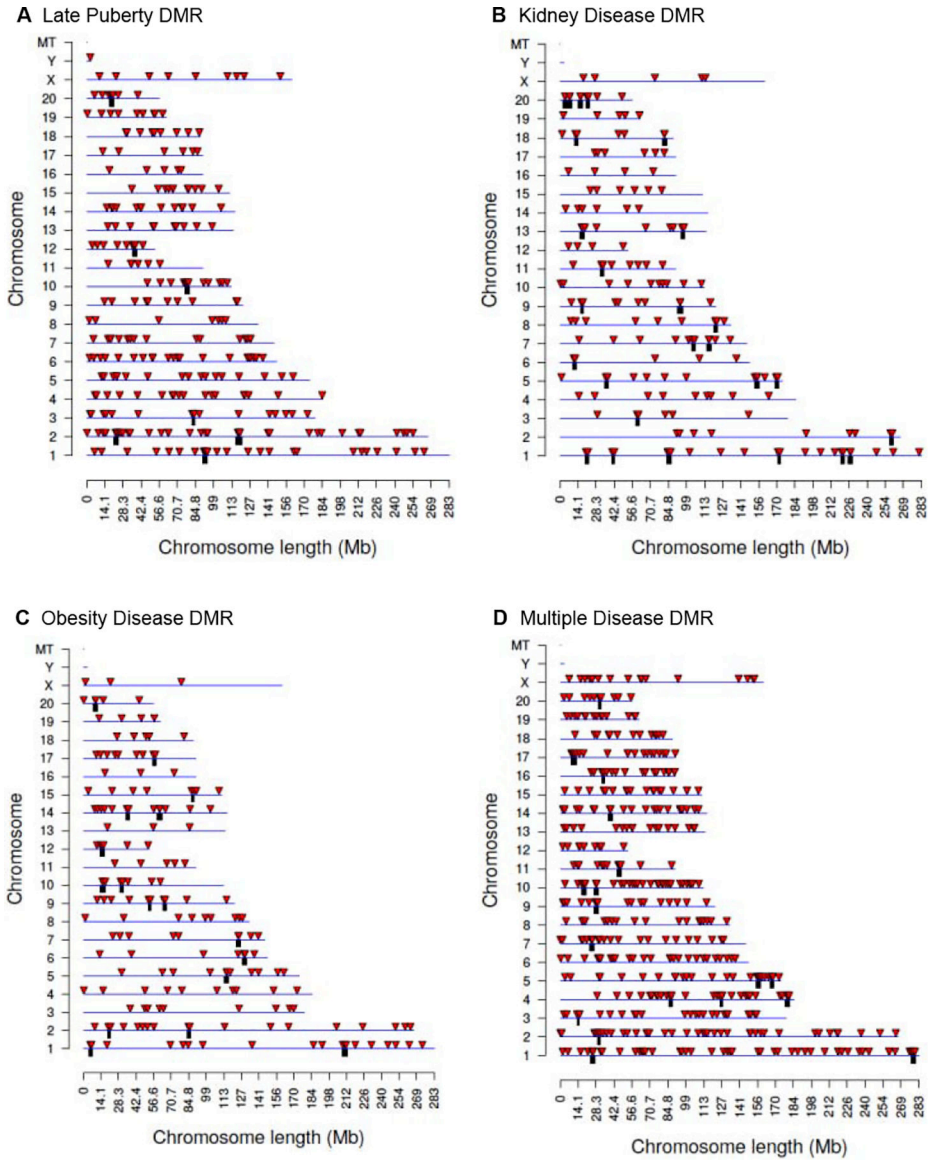

Figure 2.

DMR chromosomal locations. The DMR locations on the individual chromosomes is represented with an arrowhead and a cluster of DMRs with a black box. All DMRs containing at least one significant window at the select (bold) p-value threshold are shown. The chromosome number and size of the chromosome (megabase) are presented. **(A)** Late puberty DMRs; **(B)** Kidney disease DMRs; **(C)** Obesity disease DMRs; and **(D)** Multiple disease DMRs.

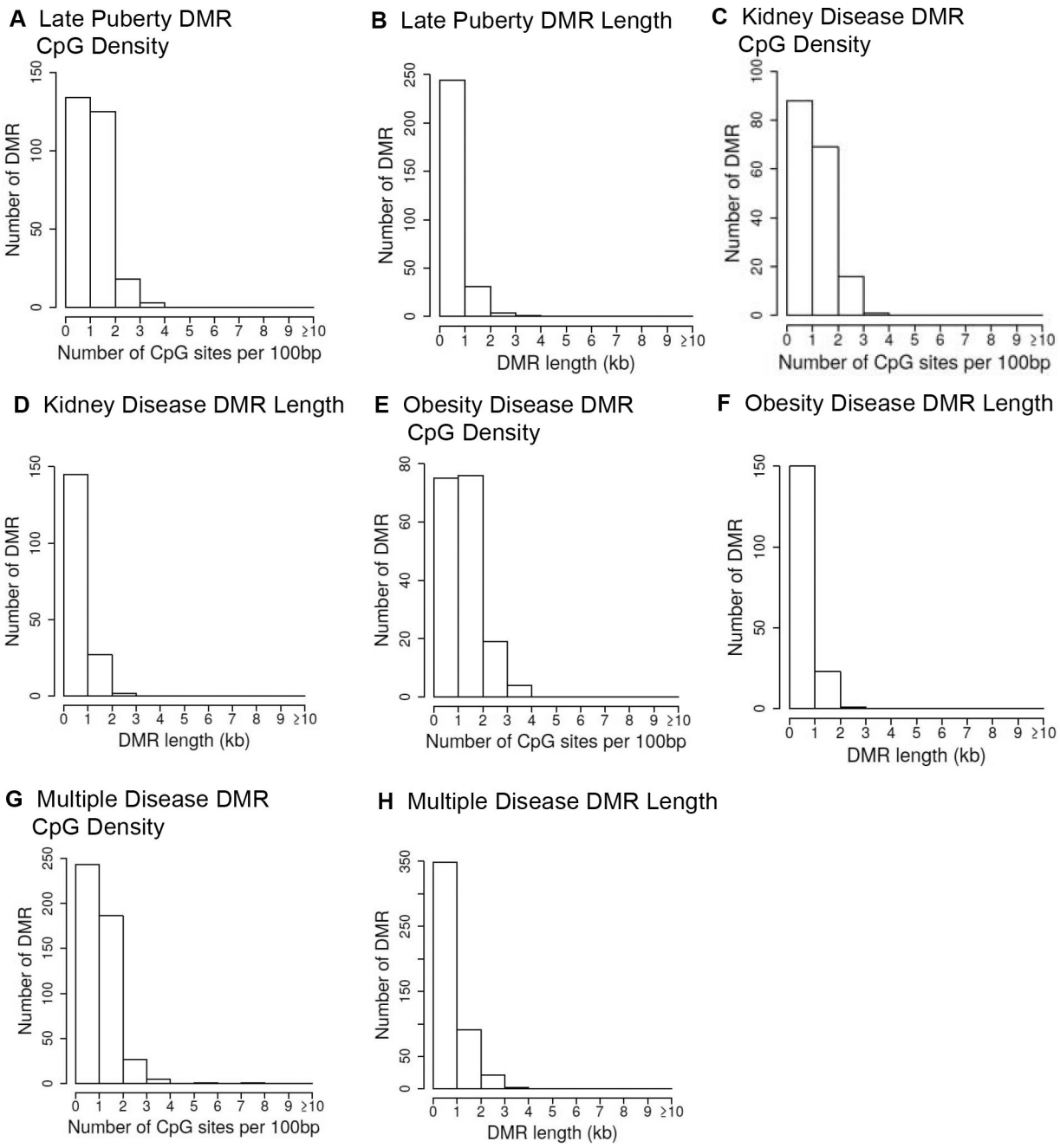

Figure 3.

DMR genomic features. The number of DMRs at different CpG densities. All DMRs at a p-value threshold of p<1e-04 are shown. **(A)** Late puberty DMR CpG density; **(B)** Late puberty DMR length; **(C)** Kidney disease DMR CpG density; **(D)** Kidney disease DMR length; **(E)** Obesity disease DMR CpG density; **(F)** Obesity disease DMR length; **(G)** Multiple disease DMR CpG density; **(H)** Multiple disease DMR length.

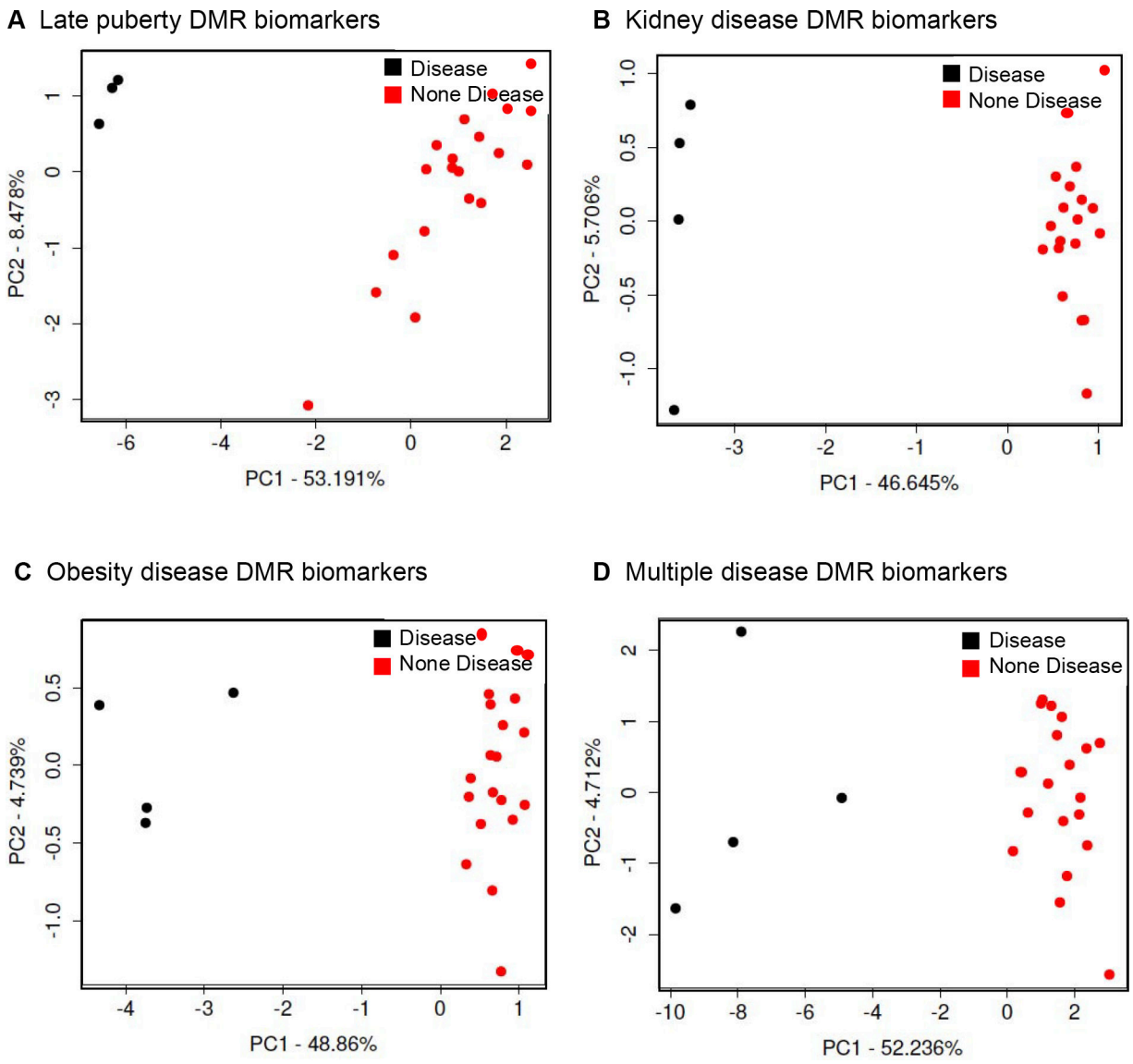

Figure 4.

DMR principal component analysis (PCA). The first two principal components are used. The underlying data is the RPKM read depth for DMR only genomic windows. **(A)** Late puberty DMRs PCA; **(B)** Kidney disease DMRs PCA; **(C)** Obesity disease DMRs PCA; **(D)** Multiple disease DMRs PCA. The color label for disease or non-disease is inserted.

A Venn Overlap Disease DMRs p<1e-04

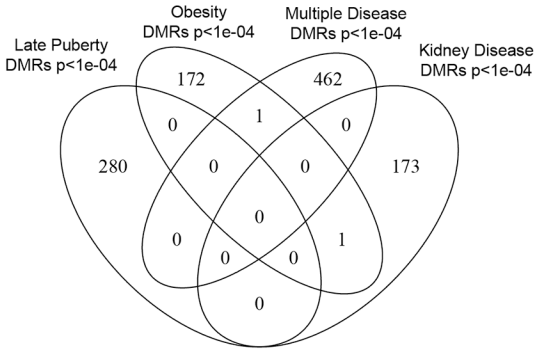

B Extended Overlap Disease DMRs

p<0.05 / p<1e-04	DMR Late Puberty	DMR Kidney Disease	DMR Obesity Disease	DMR Multiple Disease
DMR Late Puberty	280 (100.0%)	34 (12.1%)	27 (9.6%)	50 (17.9%)
DMR Kidney Disease	20 (11.5%)	174 (100.0%)	21 (12.1%)	26 (14.9%)
DMR Obesity Disease	12 (6.9%)	17 (9.8%)	174 (100.0%)	26 (14.9%)
DMR Multiple Disease	58 (12.5%)	69 (14.9%)	47 (10.2%)	463 (100.0%)

C Venn Overlap Disease DMRs p<0.05

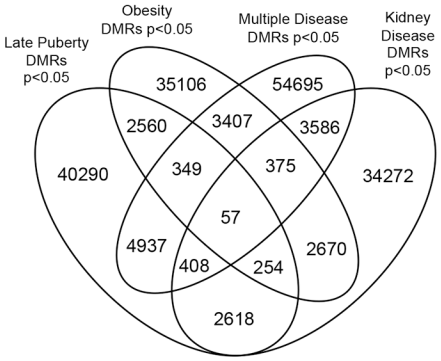

D Venn Overlap Disease DMRs p<1e-04 and Overlap DMRs p<0.05

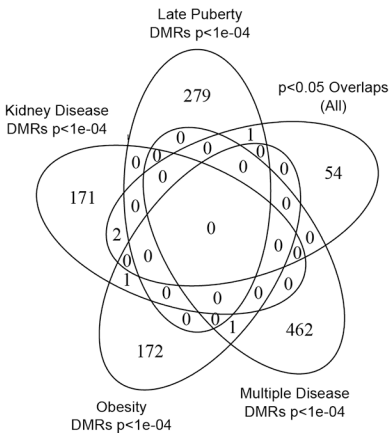

Figure 5.

Disease DMR overlap. **(A)** Venn diagram of the different disease DMRs at p<1e-04. **(B)** Extended overlap disease DMRs. The p-value data set at p<1e-04 is compared to the p<0.05 data to identify potential overlap between the different pathologies with DMR number and percentage of the total presented. **(C)** Venn diagram overlap of specific disease DMRs at p<0.05 to identify the 57 DMR overlaps in common. **(D)** Venn diagram overlap of disease specific DMRs at p<1e-04 and the p<0.05 common 57 DMR.

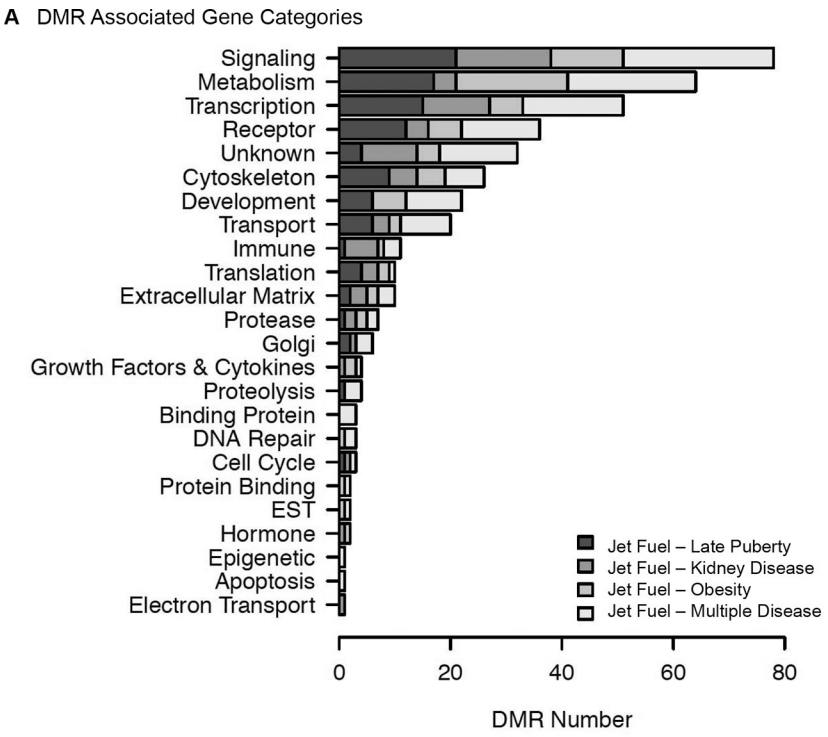

B DMR Associated Gene Pathways

Late Puberty
rno01100 Metabolic pathways (13)
rno05205 Proteoglycans in cancer (7)
rno04015 Rap1 signaling pathway (6)
rno05170 Human immunodeficiency (6)
rno04010 MAPK signaling pathway (6)

Obesity Disease
rno01100 Metabolic pathways (10)
rno05200 Pathways in cancer (8)
rno04261 Adrenergic signaling in cardiomyocytes (5)
rno05225 Hepatocellular carcinoma (5)
rno05231 Choline metabolism in cancer (4)

Kidney Disease
rno01100 Metabolic pathways (7)
rno03040 Spliceosome (4)
rno04658 Th1 and Th2 cell differentiation (3)
rno05010 Alzheimer disease (3)
rno05168 Herpes simplex virus 1 infection (3)

Multiple Disease
rno01100 Metabolic pathways (12)
rno04015 Rap1 signaling pathway (7)
rno04151 PI3K-Akt signaling pathway (7)
rno05010 Alzheimer disease (6)
rno05165 Human papillomavirus infection (6)

Figure 6.

DMR associated genes and pathways. **(A)** DMR associated gene categories. The different gene categories and number DMR presented with disease specific color index insert. **(B)** DMR associated gene pathways for each specific disease for the top five KEGG pathways and number DMR associated genes listed in bracket.

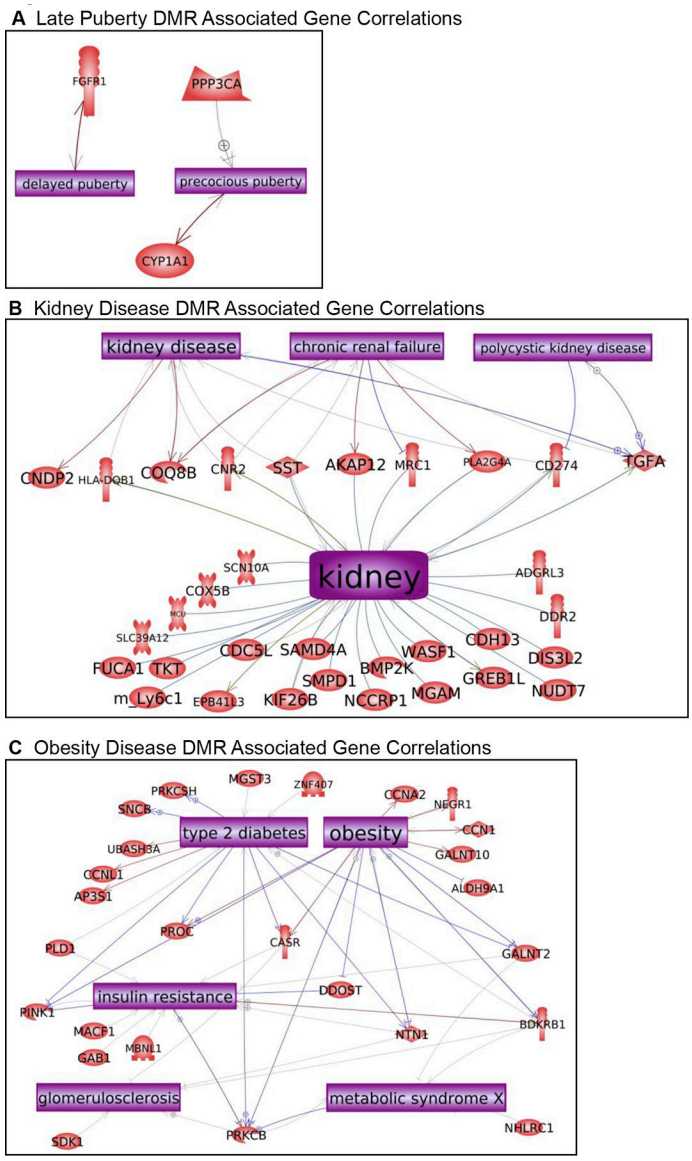

Figure 7.

DMR associated genes within the pathology biomarker DMR set for each individual pathology. The relevant tissue physiologic and pathology process is listed with direct gene links. **(A)** Late puberty, **(B)** kidney disease, and **(C)** obesity.

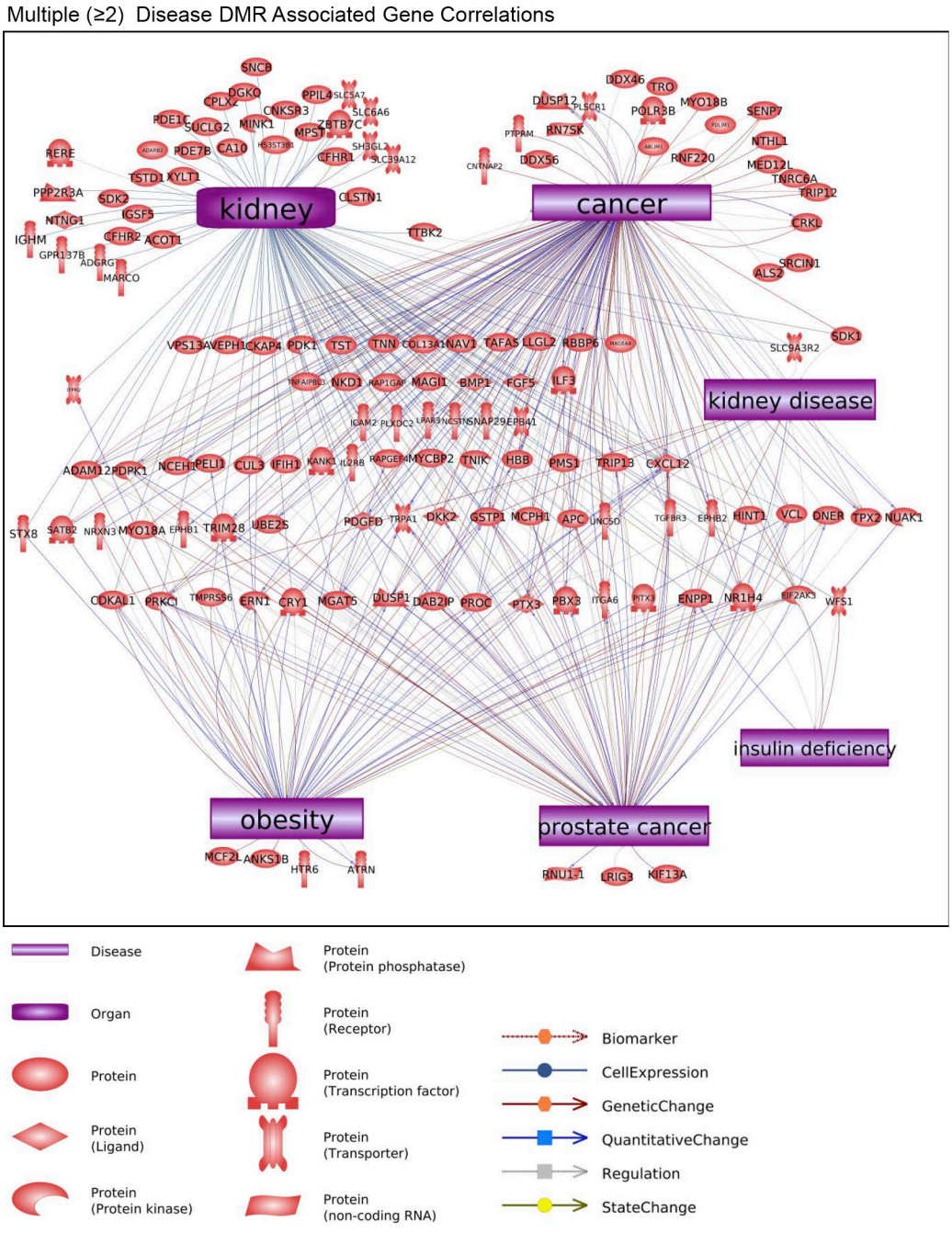

Figure 8.

DMR associated genes within the pathology biomarker DMR set for multiple disease pathology. The relevant tissue physiologic and pathology process is listed with direct gene links. The gene functional shape is presented in the inset index.

Table 1.

F3 generation jet fuel lineage male pathology. The individual animals for the jet fuel lineage males are listed and a (+) indicates presence of disease and (−) absence of disease. The animals with shaded (+) were used for the epigenetic analysis due to the presence of only one disease, except the multiple (≥2) disease. The no disease animals used were identified with a shaded (0). The ratio of number disease / total is presented and percentage with disease.

Molecular ID	Early Puberty	Late Puberty	Testis Disease	Prostate Disease	Kidney Disease	Obesity	Tumor	Multiple Disease	Total Disease
JF6	−	+	−	−	−	−	−	−	1
JF7	−	−	−	−	−	−	−	−	0
JF8	−	+	−	−	−	+	−	+	2
JF9	−	+	−	−	−	−	−	−	1
JF10	−	−	−	−	−	−	−	−	0
JF5	−	−	−	−	+	−	−	−	1
JF1	−	−	−	−	−	+	−	−	1
JF2	−	−	−	−	−	−	−	−	0
JF3	−	−	−	−	−	−	−	−	0
JF4	−	−	−	−	−	−	−	−	0
JF13	−	−	−	−	−	+	−	−	1
JF14	−	−	−	−	−	−	−	−	0
JF11	−	−	−	−	−	−	−	−	0
JF12	−	−	−	−	+	−	−	−	1
JF18	+	−	−	−	+	−	−	+	2
JF19	−	−	−	−	−	−	−	−	0
JF20	−	−	−	−	−	+	−	−	1
JF15	−	−	−	−	−	−	−	−	0
JF16	−	−	+	−	−	−	−	−	1
JF24	−	−	−	−	−	−	−	−	0
JF21	−	−	+	−	−	−	−	−	1
JF22	−	−	−	−	−	−	−	−	0
JF23	−	−	−	−	−	+	−	−	1
JF25	−	−	−	−	−	−	−	−	0
JF26	−	−	−	−	−	−	−	−	0
JF27	−	−	−	−	−	−	−	−	0
JF37	−	−	+	+	−	−	−	+	2
JF38	−	−	−	+	−	+	−	+	2
JF39	−	−	−	−	−	−	−	−	0
JF28	−	−	−	−	+	−	−	−	1
JF29	−	−	−	−	−	−	−	−	0
JF30	−	−	−	−	−	−	−	−	0

Molecular ID	Early Puberty	Late Puberty	Testis Disease	Prostate Disease	Kidney Disease	Obesity	Tumor	Multiple Disease	Total Disease
JF31	–	–	–	–	–	–	–	–	0
JF32	–	+	–	–	–	–	–	–	1
JF33	–	–	n/a	n/a	–	–	–	–	n/a
JF34	–	–	–	–	–	–	–	–	0
JF35	–	–	–	–	–	–	–	–	0
JF36	–	–	–	–	+	–	–	–	1
Totals	1/38 = 3%	4/38 = 11%	3/37 = 8%	2/37 = 5%	5/38 = 13%	6/38 = 16%	0/38 = 0%	4/38 = 11%	